Intersection of a vortex line with transverse soliton plane in rotating ^{3}He-A: π_3 topology

V. M. H. Ruutu, Ü. Parts, J. H. Koivuniemi, M. Krusius, and E. V. Thuneberg
Low Temperature Laboratory, Helsinki University of Technology, 02150 Espoo, Finland

G. E. Volovik
Landau Institute for Theoretical Physics, 117334 Moscow, Russia

(Submitted 17 October 1994)
Pis'ma Zh. Eksp. Teor. Fiz. **60**, No. 9, 659–665 (10 November 1994)

The coexistence of two continuous textures of different dimensionalities is observed in the A-phase of superfluid ^{3}He: nonsingular 4π vortex lines that cross a planar transverse soliton. The nontrivial π_3 topology of the intersection point is discussed in terms of the linking numbers. © *1994 American Institute of Physics.*

Several types of coexistence of topological defects of different dimensionalities were found in condensed matter with broken symmetry. (i) An object of lower dimensionality may serve as a boundary for a higher-dimensional object. Examples of this type are a monopole as a termination point of a disclination line in liquid crystals,[1] a cosmic domain wall with a string as its edge line,[2] an antiphase boundary terminating at a dislocation line in ordered binary alloys,[3] a planar soliton in superfluid ^{3}He-B emanating from a vortex line,[4] etc. (ii) An object of lower dimensionality may exist in a higher-dimensional object, from which it cannot escape to the world outside. Examples of this type are a Bloch line in a domain wall in ferromagnets[3] and a vortex sheet in ^{3}He-A, which is a two-dimensional soliton with accumulated one-dimensional continuous vortices.[5,6]

Here we report on an observation of another type of topological interaction: (iii) a nonsingular vortex line that crosses a transverse planar soliton (Fig. 1). In contrast with the geometry of the vortex sheet, in which the vortices are parallel to the soliton wall, in our geometry the vortex and the soliton have only zero-dimensional common region—the intersection point. The intersection represents a point-like object, which is singularity-free, since singularities are not created easily in a rotating container. Point-like continuous objects, which are usually described by the π_3 homotopy group, were discussed in many areas of physics: particle-like solitons in the phases A and B of superfluid ^{3}He (Refs. 7–9); "textures" or Skyrmions in particle physics and cosmology;[2,10] "configurations"[11,12] or "semi-defects"[13] in liquid crystals; solitons in ordered magnets,[14] etc. In all cases such an object should collapse to zero size due to energetic factors. (In some cases, however, stabilization at some length scale is suggested: this length can be produced (i) by the higher-gradient energy terms,[8] (ii) by dynamical conservation of some physical quantity which fixes the size of the soliton[7,14] or (iii) by a natural scale like the cholesteric pitch.[15] In our case the twisting of the $\hat{\mathbf{l}}$ texture within a soliton, i.e., the nontrivial π_1 topology of the soliton, together with the nontrivial π_2

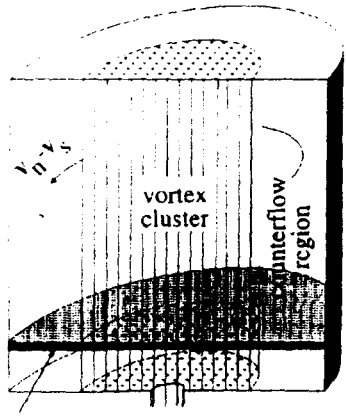

FIG. 1. A cluster of vortices crossing a transverse soliton. The cluster is surrounded by a vortex-free region with a nonzero counterflow $\vec{v}_s - \vec{v}_n$. The counterflow influences the position of the soliton peak in accordance with Fig. 3.

topology of the $\hat{\mathbf{l}}$ texture in the vortex, necessarily produce the nontrivial π_3 topology of $\hat{\mathbf{l}}$ at the intersection of these planar and linear objects.

A soliton in ^{3}He-A is a wall between domains with parallel $\hat{\mathbf{l}}=\hat{\mathbf{d}}$ and antiparallel $\hat{\mathbf{l}}=-\hat{\mathbf{d}}$ orientations of the A-phase orbital $\hat{\mathbf{l}}$ and magnetic $\hat{\mathbf{d}}$ anisotropy axes. A soliton, whose plane is oriented normal to the magnetic field direction $\mathbf{H}\|\hat{\mathbf{z}}$, is the so-called composite twist soliton, in which the $\hat{\mathbf{l}}$ and $\hat{\mathbf{d}}$ axes are twisted in opposite directions:[16] $\hat{\mathbf{l}}_{\text{soliton}}(z)=\hat{x}\cos\alpha(z)+\hat{y}\sin\alpha(z)$, $\hat{\mathbf{d}}_{\text{soliton}}(z)=\hat{x}\cos\beta(z)+\hat{y}\sin\beta(z)$, with $\alpha(+\infty)-\beta(+\infty)=\alpha(-\infty)-\beta(-\infty)+\pi$.

The soliton often appears after a cool-down to the superfluid state. Its existence is seen in cw NMR experiments as a satellite peak in the NMR absorption as a function of excitation frequency f (see Fig. 2). The frequency of an absorption maximum is conventionally expressed as $f^2=f_0^2+R^2f_\parallel^2$, where $f_0=\gamma H/2\pi$ is the Larmor frequency, and $f_\parallel$ is

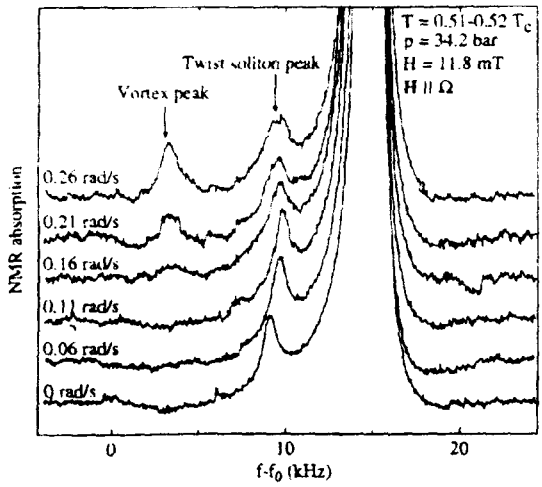

FIG. 2. cw NMR absorption as a function of the frequency shift $\Delta f=f-f_0$ from the Larmor frequency f_0 for six different rotation velocities Ω. The data are recorded in one continuous run, in which the rotation velocity is increased from zero to the maximum velocity, $\Omega_m=0.26$ rad/s, while the transverse twist soliton is in the container.

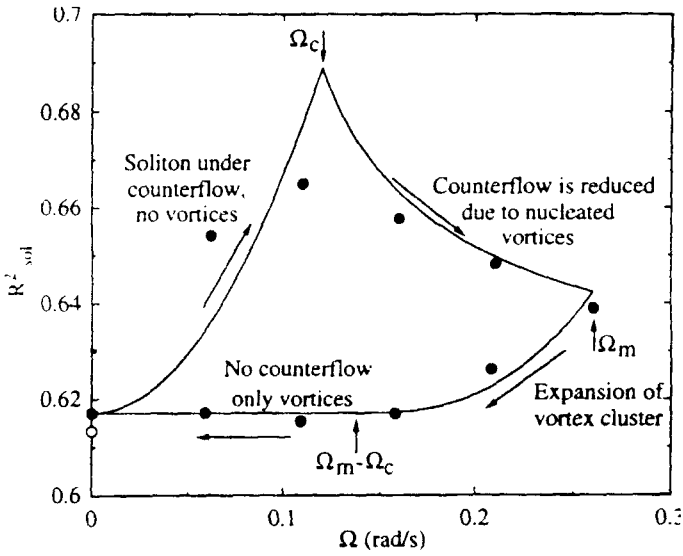

FIG. 3. (●) The normalized frequency shift R^2_{sol} of the twist soliton satellite peak versus the rotation velocity Ω, when the container is first accelerated from the stationary state to the maximum velocity, $\Omega_m=0.26$ rad/s, and then decelerated to $\Omega=0$. The initial value of R^2_{sol} is marked by (○). The hysteresis in R^2_{sol} reflects the influence of the counterflow $\vec{v}_s-\vec{\Omega}\times\vec{r}$ on the structure of the soliton. At the initial vortex-free stage, when $\vec{v}_s=0$, the counterflow increases with Ω, which leads to the initial increase of R^2_{sol}. After the critical velocity Ω_c is reached, the counterflow region decreases when a cluster of vortices is formed. As a result, R^2_{sol} decreases between Ω_c and Ω_m. During deceleration, the counterflow region shrinks further until it disappears at $\Omega=\Omega_m-\Omega_c$. At still lower Ω, i.e., in the absence of the counterflow, R^2_{sol} is nearly the same as in the stationary state. The solid line is a theoretical fit assuming that the frequency shift of the soliton peak due to the counterflow is $\propto\langle(\vec{v}_s-\vec{v}_n)^2\rangle$, averaged over the soliton. In this fit, we used for the nucleation threshold the value $\Omega_c=0.12$ rad/s. The value $\Omega_c\sim0.13$ rad/s was determined independently from the behavior of the vortex satellite.

the temperature- and pressure-dependent longitudinal resonance frequency of the A phase. The dominant peak at $R=1$ originates from the dipole-locked ($\hat{\mathbf{l}}=\pm\hat{\mathbf{d}}$) bulk liquid. The low-frequency satellite peak in the stationary container at $\Omega=0$ arises from a spin-wave mode that is localized in the core of the soliton, where the dipole-unlocked texture, $\hat{\mathbf{d}}\neq\pm\hat{\mathbf{l}}$, produces an attractive potential. The orientation of the soliton can be extracted from the position of the peak:[5] the value $R^2_{sol}=0.613$ at $\Omega=0$ is the signature of the horizontal composite twist soliton. All measurements are for the magnetic field $\mathbf{H}$ parallel to the $\hat{\mathbf{z}}$ axis of the cylindrical container at a temperature $T=0.5\ T_c$ and pressure $p=34.2$ bar. The experimental technique is the same as in Ref. 5.

In previous experiments at $T\sim0.7$–$0.8\ T_c$ the twist soliton was swept out by rotation, in contrast with the vertical soliton, which gives rise to the vortex sheet.[5] At a lower temperature $T\sim0.5\ T_c$, the transverse soliton does not disappear under rotation and remains in the container even when vortices appear. The change in the soliton structure under rotation is reflected in the dependence of R^2_{sol} on the angular velocity Ω of rotation in Fig. 3. First, the frequency shift increases, reaching the maximal value $R^2_{sol}=0.665$ at

$\Omega \sim 0.11$ rad/s and then decreases, when vortex lines start to nucleate. This is the result of interaction of the soliton with the counterflow $\vec{v}_s - \vec{v}_n$, where $\vec{v}_s$ and $\vec{v}_n = \vec{\Omega} \times \vec{r}$ are the superfluid and normal velocities, respectively.

In the acceleration–deceleration cycle of Ω in Fig. 3 four different phases are observed: (1) At first, when Ω is below the critical velocity, $\Omega_c \sim 0.13$ rad/s, of vortex nucleation, there are no vortices, and $\vec{v}_s = 0$. The counterflow $\vec{v}_s - \vec{v}_n = -\vec{\Omega} \cdot \vec{r}$ orients $\hat{\mathbf{l}}$ parallel or antiparallel to the counterflow far from the soliton. Thus the total change of $\hat{\mathbf{l}}$ across the soliton is 180°. The orientational interaction of the counterflow with $\hat{\mathbf{l}}$ leads to continuously shrinking width of the soliton wall and the dimension of the attractive potential for the spin-waves decreases. As a result, the spin-wave bound state is shifted closer to the continuum and $R^2_{\rm sol}$ increases with Ω.

(2) In the second phase, when $\Omega > \Omega_c$, vortices begin to nucleate. These are the nonsingular 4π vortices with a dipole-unlocked core,[17] which give rise to a satellite peak at $R^2_{\rm vortex} = 0.22 \pm 0.01$ (see Fig. 2). Simultaneously, $R^2_{\rm sol}$ begins to decrease, because the vorticity reduces the width of the counterflow region. This shows that when $\Omega > \Omega_c$, a cluster of vortices is formed. These vortices intersect the soliton (Fig. 1).

(3) After reaching an arbitrary maximum velocity ($\Omega_m = 0.26$ rad/s in Fig. 3), we begin to decelerate the cryostat. Now the number of vortices is conserved, while the cluster expands and the counterflow decreases in width and in magnitude. As a result, $R^2_{\rm sol}$ decreases further until the counterflow finally disappears and the cluster reaches the wall of the container. Here the initial frequency shift of the soliton peak is restored.

(4) During further deceleration, the counterflow region is absent and $R^2_{\rm sol}$ is nearly constant. This means that vortices cross an otherwise undisturbed composite twist soliton.

All four stages of this hysteretic behavior of $R^2_{\rm sol}(\Omega)$ can be reproduced theoretically (the solid line in Fig. 3) if we assume that at low counterflow velocity the dependence $R^2_{\rm sol}(\Omega)$ is analytical: $R^2_{\rm sol}(\Omega) = R^2_{\rm sol}(0) + {\rm const}\langle(\vec{v}_s - \vec{v}_n)^2\rangle$, where the average is over the rotating container. From this experiment we conclude that an intersection with continuous (nonsingular) structure exists between a vortex line and a twist soliton. It can be formed reproducibly and exists for an indefinite time as a metastable object in the rotating container.

Next we discuss the topology of the intersection of the twist soliton with the 4π vortex line along z. In the continuous 4π vortex the vorticity is produced by the nonsingular $\hat{\mathbf{l}}$ texture, which can be represented by a bound pair of Mermin–Ho (MH) 2π vortices, one with a circular and the other with a hyperbolic projection of $\hat{\mathbf{l}}$ in the xy plane (see Ref. 18, review,[17] and Fig. 4). The $\hat{\mathbf{l}}$ texture within the vortex produces the $S^2 \to S^2$ mapping with index 1: the distribution of $\hat{\mathbf{l}}$ over the cross section of circular and hyperbolic MH vortices in the xy plane covers the north and south hemispheres of the S^2 sphere $\hat{\mathbf{l}} \cdot \hat{\mathbf{l}} = 1$, respectively. The corresponding index of the $\hat{\mathbf{d}}$ texture is 0, because $\hat{\mathbf{d}}$ is kept in the xy plane by an axial magnetic field. In the vortex core $\hat{\mathbf{l}}$ and $\hat{\mathbf{d}}$ are therefore unlocked. (In a lattice of 4π vortices one has periodic boundary conditions for $\hat{\mathbf{l}}$. Thus the $\hat{\mathbf{l}}$ texture in a unit cell of the vortex lattice produces a mapping of the 2D torus, $T^2 \to S^2$, with the index 1. The whole A-phase order parameter is not periodic; it is invariant under "magnetic" translations: translations which are accompanied by a gauge transformation. As a result, the counterflow $\vec{v}_s - \vec{\Omega} \times \vec{r}$ is periodic in the vortex lattice.)

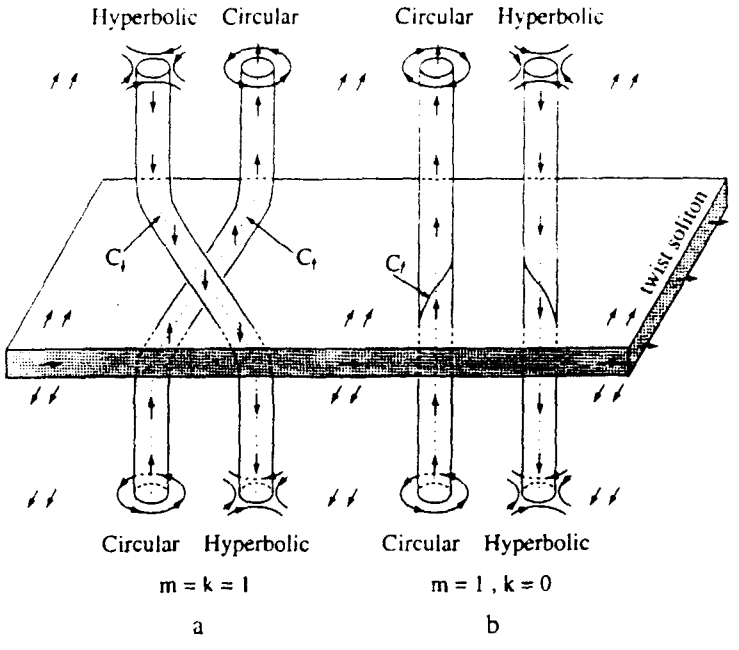

FIG. 4. Two ways for the vortex to cross the soliton. (a) Intersection with the topological indices $m=1$, $k=1$. $C_\uparrow$ and $C_\downarrow$ are loci of points, where $\hat{\mathbf{l}}$ is up and down, respectively. With two parallel twist solitons this texture can be duplicated, and the two loops form a link. (b) Intersection with indices $m=1$, $k=0$. The same linking occurs between the loop $C_\uparrow$, for which $\hat{\mathbf{l}}=\hat{\mathbf{z}}$, and a neighboring loop with constant $\hat{\mathbf{l}}\neq\hat{\mathbf{z}}$.

What happens when such a vortex crosses the soliton? Far from the vortex, i.e., in a pure soliton, $\hat{\mathbf{l}}$ is oriented in the transverse plane and its orientation depends on the vertical coordinate z: This serves as an asymptote for the intersection point, $\hat{\mathbf{l}}_{\text{asymptote}}(z)=\hat{x}\cos\alpha(z)+\hat{y}\sin\alpha(z)$. If the vortices form a lattice, then α must change exactly by π when crossing the twist soliton, because far from the soliton the vortex lattice fixes $\hat{\mathbf{l}}$ parallel or antiparallel to the lattice anisotropy axis.[17] The examples of topologically different intersections with given asymptotes far from the intersection can be embedded in the following general series with two integer parameters m and k, which will be later related to the topological invariants:

$$\hat{\mathbf{l}}_{m,k}(z,\vec{r})=\mathbf{U}^m(z)\hat{\mathbf{l}}(-\infty,\mathbf{U}^k(z)\vec{r}). \tag{1}$$

Here $\vec{r}$ is the in-plane coordinate, counted, say, from the "center of mass" of the vortex pair; $\hat{\mathbf{l}}(-\infty,\vec{r})$ is the texture within the 4π vortex far from the soliton; and $\mathbf{U}(z)$ is the z-dependent matrix, which rotates $\hat{\mathbf{l}}$ within the twist soliton:

$$\mathbf{U}(z)=\begin{pmatrix}\cos\alpha(z) & \sin\alpha(z) & 0\\ -\sin\alpha(z) & \cos\alpha(z) & 0\\ 0 & 0 & 1\end{pmatrix}. \tag{2}$$

The index m shows an algebraic sum of the solitons, while k marks two competing intersections shown in Figs. 4a and 4b. They have, respectively, $m=1$, $k=1$, and $m=1$, $k=0$ configurations. In the $m=1$, $k=1$ configuration the circular and hyperbolic MH vortices exchange places after crossing the soliton, creating an entanglement, but do not change their orientation with respect to $\hat{\mathbf{l}}_{\text{asymptote}}$. In contrast, in the $m=1$, $k=0$ configuration the MH vortices do not interchange, but each MH vortex is twisted separately. As a result, the orientation of the whole 4π vortex with respect to $\hat{\mathbf{l}}_{\text{asymptote}}$ changes to the opposite configuration. This means that the parity of the 4π vortex changes after crossing: the w^+ vortex transforms to its mirror-reflected w^- modification in the notation of Ref. 17.

This topological difference between the two textures can be described in terms of the linking numbers which usually characterize the π_3 homotopy.[19] These linking numbers are related to the indices m and k. To visualize this situation, let us consider two parallel identical solitons. This corresponds to $m=2$ and even k in Eq. (1). After crossing two solitons the 4π vortex returns to its initial $\hat{\mathbf{l}}(-\infty, \vec{r})$ texture. This means that the cylinder $V_2=T^2\times(-\infty<z<+\infty)$, which crosses two solitons, represents the 3D torus, $V_2=T^3$. Thus the $\hat{\mathbf{l}}$ texture in the cylinder produces the mapping $T^3\rightarrow S^2$. This torus homotopy has no natural group structure,[20] but can be characterized, nevertheless, by some integers.

Let us consider a loop C formed by the loci in space in which the field $\hat{\mathbf{l}}$ has a constant value. Let us use two values of $\hat{\mathbf{l}}$: one of them, $\hat{\mathbf{l}}_\uparrow$, is on the northern hemisphere and another one, $\hat{\mathbf{l}}_\downarrow$, is on the southern hemisphere. For example, $\hat{\mathbf{l}}_\uparrow=\hat{\mathbf{z}}$ and $\hat{\mathbf{l}}_\downarrow=-\hat{\mathbf{z}}$. The corresponding loops are $C_\uparrow$ and $C_\downarrow$. Let us introduce the linking number $lk(C_\uparrow,C_\downarrow)$, which counts how often $C_\uparrow$ passes through $C_\downarrow$. We find that it depends only on k; i.e., $lk(C_\uparrow,C_\downarrow)=1$ for the duplicated intersection with indices $m=1$, $k=1$ in Fig. 4a and $lk(C_\uparrow,C_\downarrow)=0$ for the duplicated intersection with indices $m=1$, $k=0$ in Fig. 4b.

Now let use consider two loops formed by loci, where $\hat{\mathbf{l}}$ takes two values on the same hemisphere (note that the $\hat{\mathbf{l}}$ texture in the circular and hyperbolic MH vortices covers the north and south hemispheres, respectively). The linking number of the two loops of type $C_\uparrow$ will then be $lk(C_\uparrow,C_\uparrow)=-lk(C_\downarrow,C_\downarrow)=1$ for the duplicated $m=1$, $k=0$ texture.

Let us express these integers in terms of analytical topological invariants. The Hopf index H, which is expressed in terms of the superfluid velocity[7]

$$H=\frac{1}{4\varkappa^2}\int_{T^3} d^3r\vec{v}_s\cdot\vec{\nabla}\times\vec{v}_s, \tag{3}$$

is not quantized in a given (open) geometry [here $\vec{v}_s=(\varkappa/2\pi)\hat{\mathbf{e}}_1\vec{\nabla}\hat{\mathbf{e}}_2$, $\Psi=\hat{\mathbf{e}}_1+i\hat{\mathbf{e}}_2$ is the complex vector order parameter with $\hat{\mathbf{e}}_1\times\hat{\mathbf{e}}_2=\hat{\mathbf{l}}$; $\varkappa=\pi\hbar/m_3$ is the circulation quantum in superfluid ^{3}He]. This occurs because the periodic boundary conditions are applied only to $\hat{\mathbf{l}}$ and $\vec{v}_s-\vec{v}_n$, but not to the whole order parameter: $\Psi(x,y,+\infty)$ is not necessarily equal to $\Psi(x,y,-\infty)$. This corresponds to a nonzero phase difference across the soliton, which is typical of Josephson contacts. The calculation of H for two identical solitons, i.e., for textures with double values of m and k, gives

$$H=\frac{1}{2}k+\frac{1}{2\varkappa}\int_{C^*} d\vec{r}\cdot\vec{v}_s, \tag{4}$$

where the last term corresponds to the phase difference and is expressed in terms of the circulation of $\vec{v}_s$ along the vertical path C^* on the lateral boundary of the cylinder. Equation (4) means that the intersections in Fig. 4a with the nonzero $k=1$ realizes the nontrivial π_3 topology.

For the intersections in Fig. 4b the index $k=0$, but the nontrivial topology of linking manifests itself in another analytical invariant, which is related to m. For the duplicated texture the circulation of $\vec{v}_s$ along the loop $C_\uparrow$ differs by one quantum from the calibrating circulation along C^*:

$$\left(\int_{C_\uparrow} - \int_{C^*} \right) d\vec{r} \cdot \vec{v}_s = +\varkappa. \tag{5}$$

Correspondingly, $(\int_{C_\downarrow} - \int_{C^*}) d\vec{r} \cdot \vec{v}_s = -\varkappa$.

Which of the two types of intersection occurs depends on the particular features of the hydrodynamic energy, and therefore on the temperature. A contribution to the energy difference between them comes from the spontaneous axial supercurrent along the vortex core caused by broken parity of the w-vortex.[17] In the texture with $m=k=1$, the vortex is in a single, say, w^+ state; therefore, the axial current does not change direction on crossing the soliton. On the other hand, in the texture with $m=1$, $k=0$ the axial current is opposite for the w^+ and w^- vortices on different sides of the solitons. The conservation law for the current requires that the intersection point should be a source or sink for the mass current which flows from the vortices via the intersection point into the bulk liquid. The flow energy can make the $m=k=1$ texture more advantageous. At present, we cannot distinguish between the two textures theoretically or experimentally.

In conclusion, the intersection of two continuous objects of different dimensionalities—the nonsingular 1D vortex and the topological 2D soliton—is experimentally concluded to exist. Two competing types of intersection, which have different indices of π_3 homotopy, are described.

This work was supported through the ROTA cooperation plan of the Finnish Academy and the Russian Academy of Sciences. G.E.V. was supported in part by the Russian Foundation for Fundamental Research, Grants 93-02-02687 and 94-02-03121; Ü.P. and V.M.H.R. received scholarships of the Finnish Cultural Foundation. G.E.V. thanks Yu. Makhlin and T. Misirpashaev for many discussions.

[1] M. Kléman, Rep. Prog. Phys. **52**, 555 (1989); I. Chuang *et al.*, Phys. Rev. Lett. **66**, 2472 (1991).
[2] A. Vilenkin, Phys. Rep. **2**, 263 (1985); A. Vilenkin and E. P. S. Shellard, *Cosmic Strings and Other Topological Defects* (Cambridge University Press, Cambridge, 1993).
[3] A. Malozemoff and J. C. Slonczewski, *Magnetic Domain Walls in Bubble Materials* (New York: Academic, 1979); Chih-Wen Chen, *Magnetism and Metallurgy of Soft Magnetic Materials* (North-Holland, Amsterdam 1977).
[4] Y. Kondo *et al.*, Phys. Rev. Lett. **68**, 3331 (1992); Phys. Rev. B **47**, 8868 (1993).
[5] U. Parts *et al.*, Phys. Rev. Lett. **72**, 3839 (1994).
[6] Ü Parts *et al.*, JETP Lett. **59**, 851 (1994).
[7] G. E. Volovik and V. P. Mineev, Zh. Eksp. Teor. Fiz. **73**, 767 (1977) [Sov. Phys. JETP **46**, 401 (1977)].
[8] R. Shankar, J. Phys. (Paris) **38**, 1405 (1977).
[9] T.-L. Ho, Phys. Rev. B **18**, 1144 (1978).
[10] J. A. Bryan *et al.*, Phys. Rev. D **50**, 2806 (1994).
[11] I. Chuang *et al.*, Science **251**, 1336 (1991).

[12] Y. Bouligand, J. Phys. (Paris) **35**, 959 (1974); Y. Bouligand *et al.*, J. Phys. (Paris) **39**, 863 (1978).
[13] R. Kutka and H. R. Trebin, J. Physique Lett. (Paris) **45**, 1119 (1984).
[14] A. M. Kosevich *et al.*, Phys. Rep. **194**, 117 (1990).
[15] R. D. Pisarski and D. L. Stein, J. Phys. (Paris) **41**, 345 (1980).
[16] K. Maki and P. Kumar, Phys. Rev. B **16**, 182 (1977).
[17] For a review on vortices in ^{3}He, see M. M. Salomaa and G. E. Volovik, Rev. Mod. Phys. **59**, 533 (1987).
[18] X. Zotos and K. Maki, Phys. Rev. B **30**, 145 (1984).
[19] H.-R. Trebin, Adv. Phys. **31**, 195 (1982); L. Michel, Rev. Mod. Phys. **52**, 617 (1980).
[20] A. T. Garel, J. Phys. (Paris) **39**, 225 (1978).

Published in English in the original Russian journal. Reproduced here with stylistic changes by the Translation Editor.